NASA Technical Memorandum 107397
AIAA–97–0049

Validation of NASA Thermal Ice Protection Computer Codes

Part 1–Program Overview

Dean Miller, Thomas Bond, and David Sheldon
Lewis Research Center
Cleveland, Ohio

William Wright and Tammy Langhals
NYMA, Inc.
Brook Park, Ohio

Kamel Al-Khalil
Cox & Company, Inc.
New York, New York

Howard Broughton
Cortez III Service Corporation
Cleveland, Ohio

Prepared for the
35th Aerospace Sciences Meeting & Exhibit
sponsored by the American Institute of Aeronautics and Astronautics
Reno, Nevada, January 6–10, 1997

National Aeronautics and
Space Administration

VALIDATION OF NASA THERMAL ICE PROTECTION COMPUTER CODES

PART 1 - PROGRAM OVERVIEW

Dean Miller
Thomas Bond
David Sheldon
NASA- Lewis Research Center

William Wright
Tammy Langhals
NYMA, Inc.

Kamel Al-Khalil
Cox & Company, Inc.

Howard Broughton
Cortez III Service Corporation

ABSTRACT

The Icing Technology Branch at NASA-Lewis has been involved in an effort to validate two thermal ice protection codes developed at the NASA-Lewis Research Center: **LEWICE/Thermal** (*electrothermal de-icing & anti-icing*), and **ANTICE** (*hot-gas & electrothermal anti-icing*). The Thermal Code Validation effort was designated as a priority during a 1994 "peer review" of the NASA-Lewis Icing program, and was implemented as a cooperative effort with industry.

During April 1996, the first of a series of experimental validation tests was conducted in the NASA-Lewis Icing Research Tunnel (IRT). The purpose of the April 96 test was to acquire experimental data to validate the **electrothermal** predictive capabilities of both LEWICE/Thermal, and ANTICE. A heavily instrumented test article was designed and fabricated to simulate **electrothermal** de-icing and anti-icing modes of operation. Thermal measurements were then obtained over a range of test conditions, for comparison with analytical predictions.

This paper presents an overview of the test, including a detailed description of (1) test article design, (2) test matrix development, (3) test procedures, and (4) validation process. Selected experimental results are presented for de-icing and anti-icing modes of operation. Finally, the status of the validation effort at this point is summarized.

NOMENCLATURE

AOA	Angle-Of-Attack (degrees)
Beta	Collection Efficiency
IRT	Icing Research Tunnel
LWC	Liquid Water Content (g/m^3)
MVD	Median Volumetric Diameter (μm)
ON/OFF	Heater On / Off Time (seconds)
Q	Heater Flux ($Watts/in^2$)
POI	Point Of Interest
RTD	Resistance Temperature Device
S	Wrap Distance (inches)
T_{evap}	Evaporative Anti-Icing Temp. (°F)
T_{wet}	Running Wet Anti-Icing Temp. (°F)
T_{tot}	Total Temperature (°F)
TTMS	Test Thermal Management System
V	Airspeed (mph)

INTRODUCTION

In 1994 the Icing Technology Branch at NASA-Lewis Research Center conducted a "peer-review" process to prioritize it's programs, based on technological needs identified by industry partners. The need for validated Thermal Ice Protection computer codes was identified as a priority, during this "peer-review" process. As a result, NASA established an experimental program to validate two NASA developed Thermal Ice Protection codes: LEWICE/Thermal (transient electrothermal de-icing & anti-icing), and ANTICE (steady-state hot-gas & electrothermal anti-icing).[1,2]

Two experimental tests comprise this validation activity. The first test utilized an airfoil with an

electro-thermal ice protection system and will be used to validate the **electro-thermal de-icing and anti-icing** predictive capability of LEWICE/Thermal, and the **electro-thermal anticing** predictive capability of ANTICE. This test was conducted in April 96, and is the subject of this paper. The second experimental test in the Thermal Code Validation effort will utilize an airfoil with a hot-gas ice protection system, and will be used to validate the **hot-gas anti-icing** predictive capability of ANTICE. This second test is currently planned for a 2-3 week time period in CY 97-98.

The Thermal Code Validation program was initially conceived as a cooperative effort to provide a close coupling between NASA-Lewis and industry during the validation process. It was felt this cooperative relationship was essential to ensure that the "validated" codes would meet the needs of the ice protection industry. For this first Thermal Code Validation test there were two categories of cooperative participation by industry partners. The first category involved providing technical advice to guide the model design, fabrication, and test plan development. The second category involved providing the actual test hardware & support, in addition to the technical participation described above. The companies involved in the first Thermal Code Validation test are listed below, along with their participation category:

- B.F. Goodrich Aerospace ... category 1
- Boeing Commercial Airplane ... category 1
- Cox & Company ... category 2
- GE Aircraft Engines ... category 1
- Rohr Industries ... category 1

This paper will provide an overview of the first Thermal Code Validation Test, conducted in the NASA-Lewis Icing Research Tunnel (IRT) in April 1996. The scope of this paper will be limited to a description of the test article design and instrumentation, test matrix development, test procedures employed, and summary of the validation process. Though some typical results will be presented, detailed comparisons between analytical predictions and experimental results are contained in the following two papers:[3,4]

"Validation of NASA Thermal Ice Protection Computer Codes: Part 2 - The Validation of LEWICE/Thermal"

"Validation of NASA Thermal Ice Protection Computer Codes: Part 3 - The Validation of ANTICE."

TEST FACILITY DESCRIPTION

Icing Research Tunnel

The experimental testing to validate NASA's Thermal Ice Protection codes was conducted in the NASA Lewis Icing Research Tunnel (IRT).[5] The NASA IRT is a closed-loop refrigerated wind tunnel. The test section is 6 ft high and 9 ft wide, and contains a turntable assembly which allows for model angle-of-attack changes. A 5000 hp fan provides airspeeds up to 400 mph (empty test section). The refrigeration heat exchanger can control the air temperature from +40 °F to -40 °F. The water spray system has been calibrated for simulating icing clouds with droplet MVD of 14 to 40μm, and Liquid Water Content (LWC) of 0.2 - 3.4 g/m^3. Figure 1 shows a schematic view of the IRT.

TEST ARTICLE DESCRIPTION

Model Description

The test article was a NACA-0012 airfoil which had a 72 inch span, and a 36 inch chord. The model was fabricated in two pieces: a leading edge section (10 inch chord), and a wooden afterbody (26 inch chord). Figure 2 is a picture of the test article installed in the IRT.

The composite leading edge was designed and fabricated by Cox & Company specifically for this test. This leading edge section had seven independently controllable heater zones as shown in Figure 3. Each heater zone had an upper and lower heating element. Both heating elements were separately controlled to the same operating setpoint. This operationally emulated a single spanwise heater zone, but provided redundancy in case a heater element should fail (which none did). The amount of thermal energy supplied to each heater zone could be independently regulated using temperature, or heat flux as the feedback control parameter.

The chordwise extent of the heater zones was established during design using Lewice's droplet impingement routine for a nominal droplet MVD of 20μm, at 100 & 200 mph airspeeds, and for a range of Angle-Of-Attack (AOA). Figure 4 is a plot of the collection efficiency (Beta) versus wrap distance (S) from the leading-edge for 0°, 2°, and 4° AOA. The impingement limits can be seen on this plot for up to 4° AOA, which was the highest AOA tested with a 20μm droplet size. The collective width of the heated zones (3.875") was chosen to extend chordwise slightly beyond the area of direct impingement. One minute

icing sprays were run in the IRT at T_{tot} = 0° F and the above conditions to confirm that the heated zones extended far enough aft on the leading-edge. Experimental results confirmed that droplet impingement was indeed within the thermally protected area of the leading- edge.

As one might expect, zone A ("parting-strip") and zones B & C would be subjected to greater water loading and larger heat transfer coefficients than heater zones farther aft on the airfoil surface (D, E, F, G). Therefore, the maximum design heat flux for heater zones A (30 W/in^2) , B (30 W/in^2), & C (30 W/in^2) was greater than for zones D (27 W/in^2), E (27 W/in^2), F (16 W/in^2), & G (16 W/in^2). These design values represented the maximum heat flux that could be supplied to a particular zone. The actual heat flux applied to a particular zone varied depending on the test conditions, but in general was less than the maximum value.

Guard heaters were also employed to minimize spanwise heat flow within the test article. The guard heaters were physically located above and below the test area, which had a spanwise extent of approximately +/- 18 inches about the model centerline. The guard heaters were set to a nominal operating temperature based on the observed surface temperatures within the test area.

A cross-sectional view of the leading-edge composite structure is shown in Figure 5, along with thermal properties. The stainless steel abrasion shield was the outermost layer and therefore exposed to the icing environment. Note that the heater element is represented as a thin layer having equivalent cross-sectional surface area as that of the electrical conductors in the heating element. This representation is consistent with the modeling of the electrical heating elements in LEWICE/Thermal and ANTICE. A relatively thick layer of insulation formed the innermost layer of the composite structure, and helped to minimize heat flow back into the interior of the test article.

Instrumentation Design

The primary method for validating the thermal ice protection codes was planned to be via comparison of measured and predicted temperature profiles within the leading-edge structure. This validation approach was the dominant factor in designing the instrumentation layout.

A "benchtest" of the planned instrumentation design was conducted prior to fabrication of the composite leading-edge. A 6 inch by 6 inch representation of the composite leading-edge, including heater and instrumentation, was fabricated and tested. The "benchtest" was intended to verify the accuracy of the temperature measurement approach, as well as identifying any potential fabrication issues early in the design process. The "benchtest" results verified the instrumentation design approach, but indicated a potential problem associated with the heat flux gage leadwires which will be discussed later in this section.

Figure 6a shows the instrumentation layout with the leading-edge unwrapped. Note that there were 14 sensor locations (2 locations per heater zone) positioned within 4.5 inches of the test article centerline. This was done to ensure that the sensor locations would be unaffected by any potential end effects occurring at the edges of the Test Area (+/- 18 inches above and below the centerline). Also, each sensor location was centered within it's respective heater zone (in the direction parallel to the chord line).

An infrared camera was also used to obtain a temperature map of a portion of the test area as shown in Figure 6a. This long-wave infrared camera was cooled with a Stirling cycle engine, and had a scanning system with a 8-12 micron spectral response.

Since the abrasion shield of the test article was constructed of polished stainless steel, it emitted only 2% and reflected close to 98% of the ambient radiant energy. To eliminate the reflections, the region of interest was spray painted flat black. This raised the emissivity, and reduced the reflections. The camera system was calibrated using electrical tape with a known emissivity which showed that the flat black paint increased the emissivity of the surface to 97%.

The IR camera was fitted with a 40 degree, medium telephoto lens providing a field of view which captured the upper portion of the heater zones shown in Figure 6a. Six points of interest (POI) were selected in the upper portions of zones B, D, F. The temperature at each POI was averaged to provide a smooth temperature plot as a function of time.

During a run, the IR camera would capture one image every second for the duration of the run and write those images to the hard drive of the system controller. Concurrent with the image capture, the six POI temperatures were plotted in real time on the monitor, and the last thousand POI temperature data points saved to the hard drive for later analysis.

Since this was the first time NASA used this camera in an icing test, it was decided not to utilize it as a primary temperature measurement for validation purposes. It did, however, provide an independent check on the outer temperature measurement described above, and provided valuable qualitative information about the uniformity of the surface temperature within the test area.

A cross-sectional view at a typical sensor location is also shown in Figure 6b. There were 3 temperature sensors and a heat flux gage within each sensor location. Note that the temperature sensors were located so as to provide a transverse temperature profile (i.e.-axis normal to the surface) for comparison with code predictions. Some details about each sensor are provided below:

- A type T thermocouple was welded to the underside of the stainless steel abrasion shield. Since the abrasion shield was only .008 inches thick, this temperature measurement should be very near the actual surface temperature

- An RTD was located just under the heater element to obtain a temperature measurement near the heater. Though the temperature measured at this location is somewhat less than the actual heater temperature, it does provide some indication as to the magnitude of the heater temperature.

- A type T thermocouple was welded to a small stainless steel tab which was then attached to the underside of the insulation layer with a thermally conductive cement.

- The heat flux gage was a thermopile type enclosed in a polyimide film with relatively large leadwires (.010 inch diameter). Originally, it had been planned to locate the heat flux gage above the heater element, but just below the abrasion shield. However, there was a potential for air voids to form around the heat flux gage leadwires during the fabrication process. Since these air voids could lead to overheating and failure of the heating element beneath the voids, it was decided to move the heat flux gage below the heater as shown in Figure 6b. In this position, the absolute magnitude of the heat flux gage signal was greatly reduced (over a factor of 20), since almost all of the thermal energy flows from the heater outward through the abrasion shield.

Measurement Uncertainty:

The 3 test article temperature measurements described above were intended to serve as a reference against which the "goodness" of the analytical predictions would ultimately be judged. Therefore, it was important to have an estimate of the uncertainty associated with each temperature measurement. In an attempt to estimate this uncertainty, three potential uncertainty factors were considered:

1. Positional uncertainty (i.e.- how well is the sensor's actual position really known?)
2. Measurement uncertainty introduced by the data acquisition process
3. Uncertainty due to the sensor's inherent accuracy

Temperature errors due to positional uncertainty were only estimated for the transverse direction within the leading-edge structure for each of the 3 sensors. While it is recognized that this type of uncertainty has a three dimensional aspect, temperature error due to positional uncertainty in the chordwise or spanwise directions was assumed to be negligible when compared to temperature errors due to positional uncertainty in the transverse direction. It was possible to estimate a temperature uncertainty based on the following: (1) knowledge of the material properties in the immediate vicinity of the sensor, (2) an assumed nominal heat flux, and (3) an estimate of how much the transverse position could be in error. Considering the foregoing, temperature uncertainty estimates were calculated for the abrasion shield thermocouple, RTD, and insulation thermocouple at 3 nominal heater fluxes. These values are listed in Table I for nominal applied heater fluxes of 5 to 15 watts/in^2.

Measurement uncertainty due to the data acquisition process was estimated to be a fixed percentage of the data system input stage full-scale range. This uncertainty was estimated to be 0.5% for a thermocouple input (+/-5mV Full-Scale range), and 1.0% for the RTD input (+/- 1V Full-Scale range). This translates to +/- 1.0°F for the thermocouples, and +/- 1.6°F for the RTD.

Uncertainty due to inherent temperature sensor accuracy was determined based on oil bath calibrations of a random sample of Type T thermocouples and RTDs similar to those used in the test article. The thermocouples had an uncertainty of +/- 0.1°F, while the RTD uncertainty was determined to be +/- 1.9°F.

An overall value of temperature uncertainty was determined for each of the three temperature sensors by calculating the root-sum-square of the previously determined uncertainties, as shown in Table I.

TEST MATRIX

Development of the test matrix involved the selection of two different types of parameters: icing parameters (T_{tot} , LWC, MVD, etc), and electro-thermal ice protection system parameters (heater power level, and heater zone ON/OFF time). The combination of both sets of parameters resulted in an extremely large number of possible test parameter combinations for potential inclusion in the test matrix. Consequently, it was decided to restrict testing to a few different icing conditions (i.e.- limit the number of icing parameter combinations), but thoroughly evaluate the ice protection system parameters at each of these selected icing conditions.

Icing Condition Parameter Selection

Two icing test conditions were selected based on the criteria that they were: (1) generally representative of a thermal ice protection system design point, (2) reproducible by the IRT spray system, and (3) within the FAR-25 icing envelope.

- T_{tot} = 20°F, V=100mph, LWC=.78 g/m^3, MVD=20μm, AOA=0°
- T_{tot} = 0°F, V=100mph, LWC=.78 g/m^3, MVD=20μm, AOA=0°

These two conditions were given the label of "anchor point". At each of these two icing conditions, ice protection system parameters were varied. This enabled the ice protection codes' predictive capabilities to be thoroughly evaluated with respect to a reference icing condition (i.e.- an "anchor point"). Additional icing conditions were also selected to validate both codes' predictive capability at other points within the FAR-25 envelope. However, ice protection system parameters were not varied at these conditions. A list of icing test conditions is contained in Table II.

Ice Protection System Parameter Selection

The primary parameters to be considered were the heat flux (Q) applied to each heater zone, and the time sequencing of Q to each zone (ON/OFF time). Typically, higher Q was applied to the forward heater zones; therefore, the applied Q differed between zones for both De-Icing and Anti-Icing modes of operation. The same ON/OFF time cycle was applied to each individual heater zone during De-Icing operation (except heater zone A which was ON continuously). In the case of Anti-Icing operation, all heater zones were ON continuously.

Prior to the test, LEWICE/Thermal and ANTICE were used to estimate the Q values and ON/OFF times required for the validation testing. Because it was not known how appropriate these values would be, the first experimental test runs in the IRT were allocated to "exploring" the validity of these predictions. Therefore, these test runs were labeled "exploratory runs", and were not considered part of the actual validation process. These exploratory test runs indicated that initial De-Icing ON/OFF time predictions required some adjustment (shorter ON times and longer OFF times). Additionally, these test runs facilitated the fine tuning of both the De-Icing and Anti-Icing operational procedures which will be described in the next section. A list of heater Q and ON/OFF times is given in Table III for the De-Icing mode of operation. A list of T_{evap} and T_{wet} is given in Table IV for Anti-Icing operation.

EXPERIMENTAL PROCEDURES

An important part of the validation process involved the development of experimental procedures. This was necessary not only to ensure consistency in execution of the validation tests, but also to provide a means of later reconstructing how the test was actually conducted. Two distinct procedures were developed: one for De-Icing tests, and another for Anti-Icing tests.

Both of these procedures make reference to the TTMS (Test Thermal Management System) which was developed by Cox & Company to conduct thermal ice protection system testing. The TTMS performed the combined function of a data acquisition system, and a heater power distribution/control system. It was utilized to acquire all of the thermal sensor data from the test article, as well as provide closed-loop power control to all of the heater elements on the test article.

De-Icing Test Procedure

- Select icing tunnel T_{tot}, airspeed, and spray conditions
- Start fan and allow tunnel to reach temperature and airspeed setpoint
- Select ON/OFF time and program into TTMS
- Select heater flux (Q) for each of the 7 heater zones, and program into TTMS
- Setup TTMS so as to provide that Q to each heater zone (constant Q mode)

- Simultaneously, perform the following:
  - ⇒ Initiate icing spray
  - ⇒ Initiate heater cycling sequence starting with OFF time
  - ⇒ Start data acquisition process
  - ⇒ Start video & Infra-Red camera recording process
- After 5 de-icing cycles, stop spray, heater cycling, data acquisition, and video recording
- Stop fan, and enter tunnel to take photographs and rivulet measurements
- Clean ice from test article & go to next condition

In the De-Icing mode of operation, the parting strip was ON continuously. The very first heater cycle was initiated (simultaneously with the start of the icing spray) by waiting a period of time equal to the OFF time. Then power was simultaneously applied to zones B&C for the ON time. Immediately after the ON time had elapsed for zones B&C, power was simultaneously applied to zones D, E, F, &G for the ON time. After waiting for the OFF period of time (relative to zones B&C), the entire sequence then repeated itself. This typical heater zone sequence is illustrated in Figure 7, for an ON / OFF time sequence of 10 seconds ON / 110 seconds OFF.

Anti-Icing Test Procedure

- Select icing tunnel T_{tot}, airspeed, and spray conditions
- Start fan and allow tunnel to reach temperature and airspeed setpoint
- Select evaporative surface temperature (T_{evap}), and program into TTMS
- Setup TTMS to control each heater zone to T_{evap}, using the abrasion shield temperatures to sense Tevap (constant Temperature mode)
- Initiate TTMS controlled application of heat to the test article in constant Temperature mode
- Initiate icing spray
- When abrasion shield temperatures stabilize at T_{evap}, switch to constant Q mode
- Set Q to value given by constant Temperature mode of operation, then adjust Q until abrasion shield sensors in each heater zone indicate T_{evap}
- Then perform the following:
  - ⇒ Start data acquisition process
  - ⇒ Start video & Infra-Red camera recording process
- After 10 minutes or other specified time, stop spray, turn off heater power, stop data acquisition, and video recording
- Stop fan, and enter tunnel to take photographs and rivulet measurements
- Now repeat all the previous steps at T_{wet} instead of at T_{evap}
- Clean ice from test article, & go to next condition

In the Anti-Icing mode of operation, power was applied to all heater zones continuously.

RESULTS

Typical temperature sensor results are shown in Figure 8 for a De-Icing test run, and Figure 9 for a "running wet" Anti-Icing test run. These figures show a time-history of the transverse temperature profile measured within a particular heater zone. Three temperature traces are shown in each plot:

1. **Outer** temperature - measured by the abrasion shield thermocouple (very close to actual surface temperature)
2. **Middle** temperature - measured by an RTD (indicated lower value than the actual heater temperature, but considered an approximate representation of the heater temperature)
3. **Inner** temperature - measured by a thermocouple on the inner surface of the insulation (representative of insulation temperature)

During the course of testing, it was noticed that one side of the test article (C, E, G) exhibited more frozen rivulets aft of the heater zones, than did the other side (B, D, F). Upon investigation, it was determined that during the fabrication process, the heater zones had all been slightly shifted toward the side with heater zones C, E, & G by 0.1875 inches. This shift had a significant effect on the parting strip heater (zone A), which was originally centered with 0.375 inches on each side of the hi-lite. The fabrication shift placed 0.1875 inches of heater zone A to the (B, D, F) side of the hi-lite, and 0.5625 inches to the (C, E, G) side of the hi-lite. This resulted in more thermal energy being imparted to the impinging water on side (C, E, G), than side (B, D, F). This additional energy resulted in more frozen runback beyond the aft heater zones E&G.

Photos of frozen runback on both sides of the test article are shown for a De-Icing test run in Figure 10. These photos were obtained at the end of a De-Icing run at icing test condition 2, which had a relatively high LWC of 1.1 g/m^3 (V= 100 mph). This condition was chosen, because the high LWC better illustrates that there was more runback on the side with heater

zones (C, E, G). Since the majority of the validation tests were conducted at a LWC of .78 g/m^3 (V=100mph), the difference in runback was not this pronounced.

VALIDATION PROCESS

To account for the test article heater shift, the computer code input geometry files were specified to reflect the actual heater zone locations. LEWICE/Thermal and ANTICE predicted temperature profiles were then compared with the measured temperature profiles.

The primary method for validating LEWICE/Thermal and ANTICE was via comparison of experimentally measured and predicted temperatures within the leading-edge structure. As shown in Figure 6, there were sensor locations within each of the 7 heater zones. At each of these locations, temperature sensors were installed within the heater layup to provide a transverse temperature profile at that location. It is the measurements from these sensors that will be utilized to validate the transient predictive capability of LEWICE/Thermal, as well as the steady-state predictive capability of ANTICE. A full discussion of the results of these comparisons is beyond the scope of this paper, but will be given in references 3 and 4.

SUMMARY

The first in a series of NASA Thermal Code Validation tests was successfully completed. A large experimental database was generated using a test article with an electro-thermal ice protection system. Thermal data were acquired over a range of icing and ice protection system parameters for the purpose of validating the electro-thermal predictive capabilities of LEWICE/Thermal and ANTICE. The validation was accomplished via the direct comparison of experimental and predicted temperatures.

A slight misalignment of the heater zones was identified during validation testing. All heater zones were shifted by .1875 inches toward the side with heater zones C, E, & G. This resulted in more frozen runback aft of the heater zones on side (C, E, G). The validation process accounted for this by modeling the shift, and then comparing the "heater shifted" temperature predictions with experimental measurements.

The code versions validated were LEWICE/Thermal version 1.7 and ANTICE version 1.B. Detailed comparisons of experimental and predicted results are contained in the following reports:

"Validation of NASA Thermal Ice Protection Computer Codes: Part 2 - The Validation of LEWICE/Thermal"
"Validation of NASA Thermal Ice Protection Computer Codes: Part 3 - The Validation of ANTICE."

Future plans include compilation of the Thermal Code Validation Data on a CD-ROM. This CD-ROM will contain: "raw" data and index, validated versions of LEWICE/Thermal and ANTICE, Thermal Code Validation reports, and detailed results from selected comparisons of experimental data and code predictions.

ACKNOWLEDGEMENTS

Completion of the first Thermal Code Validation test was made possible by the collective efforts of many individuals. The authors would like to express their appreciation to:

- Cox & Company, Inc. for designing and fabricating the test article
- Each of the industry partners for providing technical guidance
- The Icing Research Tunnel crew for their technical support and operation of the icing tunnel
- Mr. Charles Andracchio and Ms. June Thompson for configuration and programming of NASA's ESCORT data acquisition system
- Mr. Jay Owens, and Mr. James Sims for their photographic imaging expertise, and operation of the Infra-Red camera system
- The NASA Icing Technology Branch for analytical and experimental technical support

REFERENCES

1. Masiulaniec, K.C., Wright, W.B., Users Manual for the NASA Lewis Ice Accretion / Heat Transfer Prediction Code with Electro-Thermal De-Icer Input , NASA CR-4530, July 1994.

2. Al-Khalil, K.M., Development of an Anti-Icing Runback Model, AIAA Paper 90-0759, January 1990.

3. Wright, W.B., Al-Khalil, K.M., Miller, D.R., "Validation of NASA Thermal Ice Protection Computer Codes: Part 2 - The Validation of LEWICE/Thermal", AIAA Paper 97-0050, January 1997.

4. Al-Khalil, K.M., Wright, W.B., Miller, D.R., "Validation of NASA Thermal Ice Protection Computer Codes: Part 3 - The Validation of ANTICE", AIAA Paper 97-0051, January 1997.

5. Soeder, R.H., Sheldon, D. W., Andracchio, C. R., Ide, R.F., Spera, D.A., Lalli, N.M., NASA-Lewis Icing Research Tunnel Users Manual, NASA TM-107159, June 1996.

Table I. Temperature Measurement Uncertainty

	Positional Uncertainty (for nominal heater Q)		Data Acquisition Uncertainty	Sensor Uncertainty	Total Uncertainty
Abrasion Shield Thermocouple	$Q=5w/in^2$	+/- 1.4 °F	+/- 1.0 °F	+/- 0.1 °F	+/- 1.7 °F
	$Q=10w/in^2$	+/- 2.8 °F			+/- 2.9 °F
	$Q=15w/in^2$	+/- 4.2 °F			+/- 4.3 °F
RTD	$Q=5w/in^2$	+/- 0.4 °F	+/- 1.6 °F	+/- 1.9 °F	+/- 2.5 °F
	$Q=10w/in^2$	+/- 0.8 °F			+/- 2.6 °F
	$Q=15w/in^2$	+/- 1.3 °F			+/- 2.8 °F
Insulation Thermocouple	$Q=5w/in^2$	+/- 1.5 °F	+/- 1.0 °F	+/- 0.1 °F	+/- 1.8 °F
	$Q=10w/in^2$	+/- 2.9 °F			+/- 3.1 °F
	$Q=15w/in^2$	+/- 4.4 °F			+/- 4.5 °F

Table II. Icing Conditions Tested

Icing Condition	T_{tot} (°F)	V (mph)	LWC (g/m^3)	MVD (μm)	AOA (degrees)
1	20	100	.78	20	0
2	20	100	1.1	20	0
3	20	200	.39	20	0
4	0	100	.78	20	0
5	0	100	1.1	20	0
6	0	200	.39	20	0
7	20	200	.55	20	0
8	0	200	.55	20	0
9	20	100	.78	20	-2
10	20	100	.78	20	-4
11	20	100	.90	40	0
12	-22	200	.39	20	0
13	15	100	2.0	20	0
14	0	100	.78	20	-2
15	0	100	.78	20	-4

Table III. Nominal Ice Protection System Parameters Tested- (De-Icing Mode)

Icing Condition	Test Run Numbers	T_{tot} (°F)	Heater ON/OFF Time (seconds)	$Q_{zone\ A}$ (Watt/in^2)	$Q_{zones\ B,C}$ (Watt/in^2)	$Q_{zones\ D,E}$ (Watt/in^2)	$Q_{zones\ F,G}$ (Watt/in^2)
1	18-20, 24-26, 28-30	20	10/110, 7/113, 5/115 " "	5 5 5	8 10 7	8 8 7	8 8 7
2	45-47	20	10/110, 7/113, 5/115	5	7	7	7
3	50-52	20	10/110, 7/113, 5/115	7	10	10	10
4	32-34 37-39 41-43	0	10/110, 7/113, 5/115 " "	10-12 12 12	12 16 14-20	10-14 16 14-15	10-12 15 14-15
5	55-57	0	10/110, 7/113, 5/115	12	16	16	15
6	60-62	0	10/110, 7/113, 5/115	15	20	20	15
7	64	20	10/110	7	10	10	10
8	66	0	10/110	15	20	20	15
9	68	20	10/110	5	8	8	8
10	70	20	10/110	5	8	8	8
11	72	20	10/110	5	8	8	8
12	74	-22	10/110	25	30	30	15
13	86	15	10/110	7	10	10	10
14	88	0	10/110	12	16	16	15
15	90	0	10/110	12	16	16	15

Table IV. Nominal Ice Protection System Parameters Tested- (Anti-Icing Mode)

				Nominal Surface Temperatures, (°F)			
Icing Condition	Test Run Number	T_{tot} (°F)	Anti-Icing Mode of Operation	Zone A	Zones B,C	Zones D,E	Zones F,G
1	22	20	Evaporative Running Wet	115 38	150 38	150 38	150 38
2	48	20	Evaporative Running Wet	120 37	160 39	160 39	160 39
3	53	20	Evaporative Running Wet	95 38	100 38	100 38	100 38
4	35	0	Evaporative Running Wet	115 35	150 37	150 37	150 35
5	58	20	Evaporative Running Wet	115 40	155 40	155 40	155 40
6	63	20	Evaporative Running Wet	100 45	100 45	100 45	100 45
7	65	20	Evaporative Running Wet	105 39	135 39	135 39	135 39
8	67	0	Evaporative Running Wet	90 44	95 44	95 44	95 40
9	69	20	Evaporative Running Wet	115 40	155 40	155 40	155 38
10	71	20	Evaporative Running Wet	115 40	155 40	155 40	150 40
11	73	20	Evaporative Running Wet	115 42	150 42	150 42	150 40
12	75	-22	Evaporative Running Wet	95 50	120 56	120 56	115 52
13	87	15	Running Wet	40	40	40	38
14	89	0	Evaporative Running Wet	110 47	170 47	170 47	170 45
15	91	0	Evaporative Running Wet	120 40	160 44	160 44	160 44

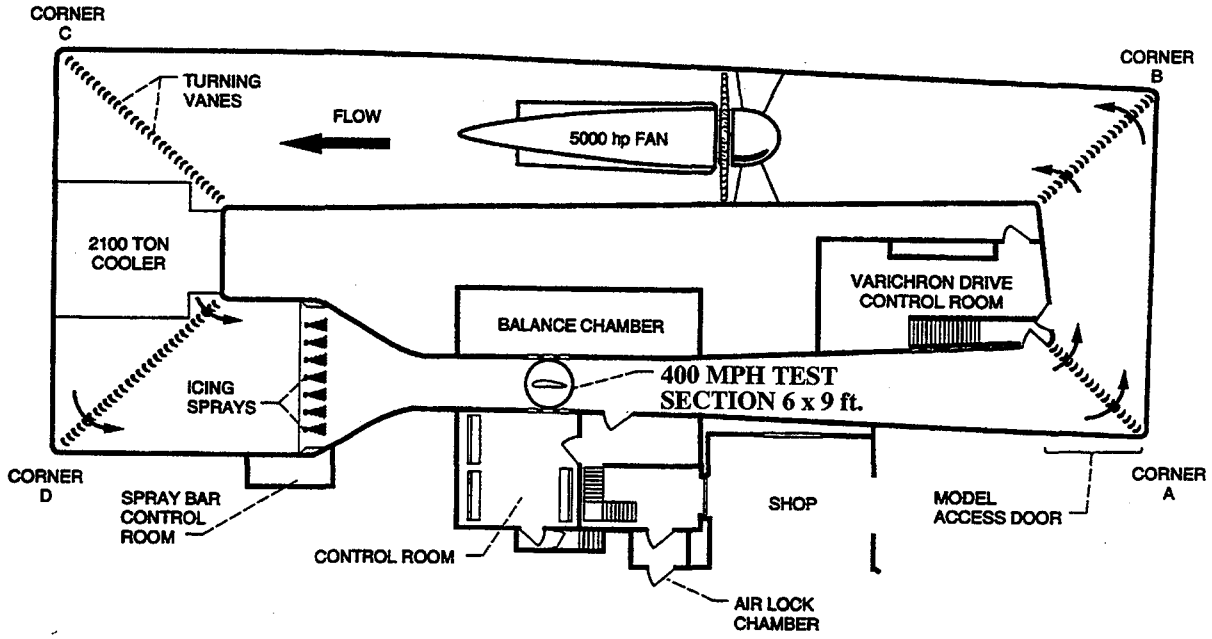

Figure 1 – Plan view of Icing Research Tunnel.

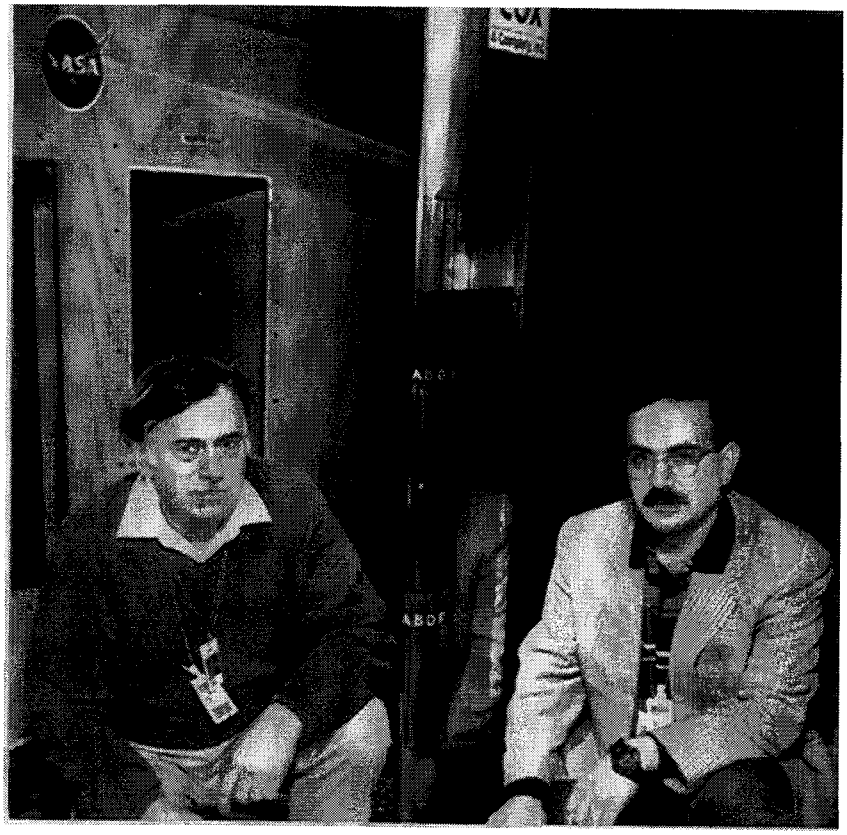

Figure 2 – Test article installed in Icing Research Tunnel

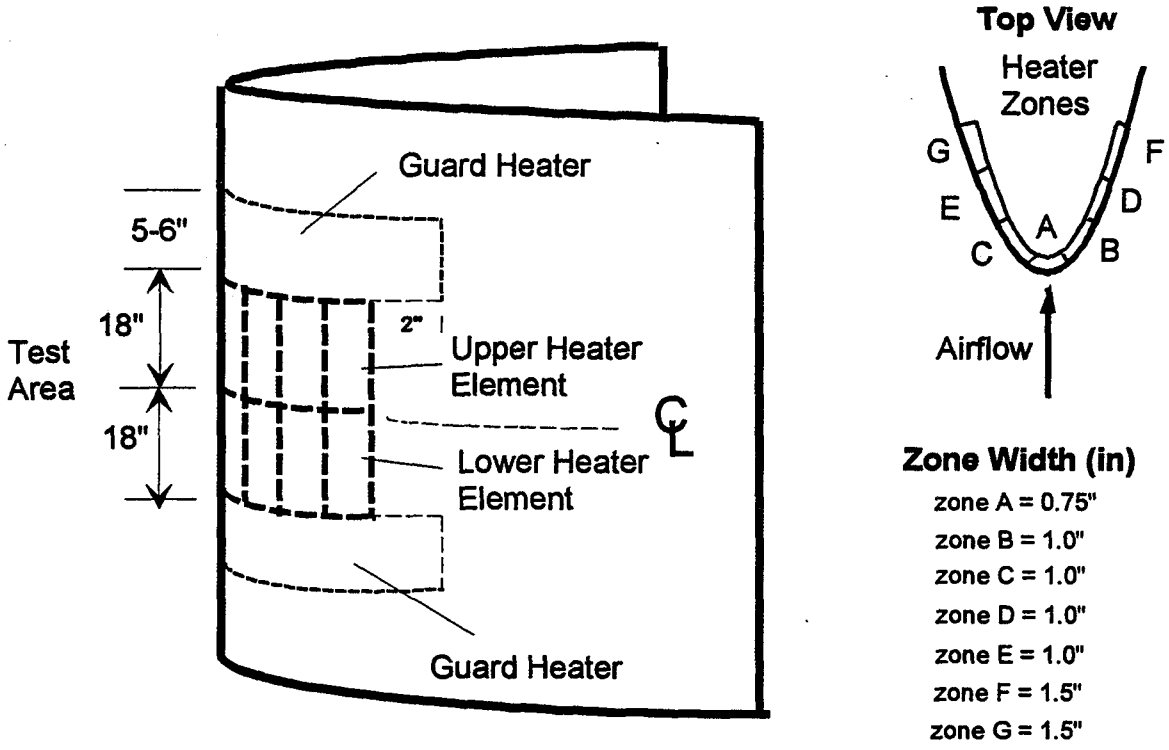

Figure 3 - Test article electro-thermal heater zone layout.

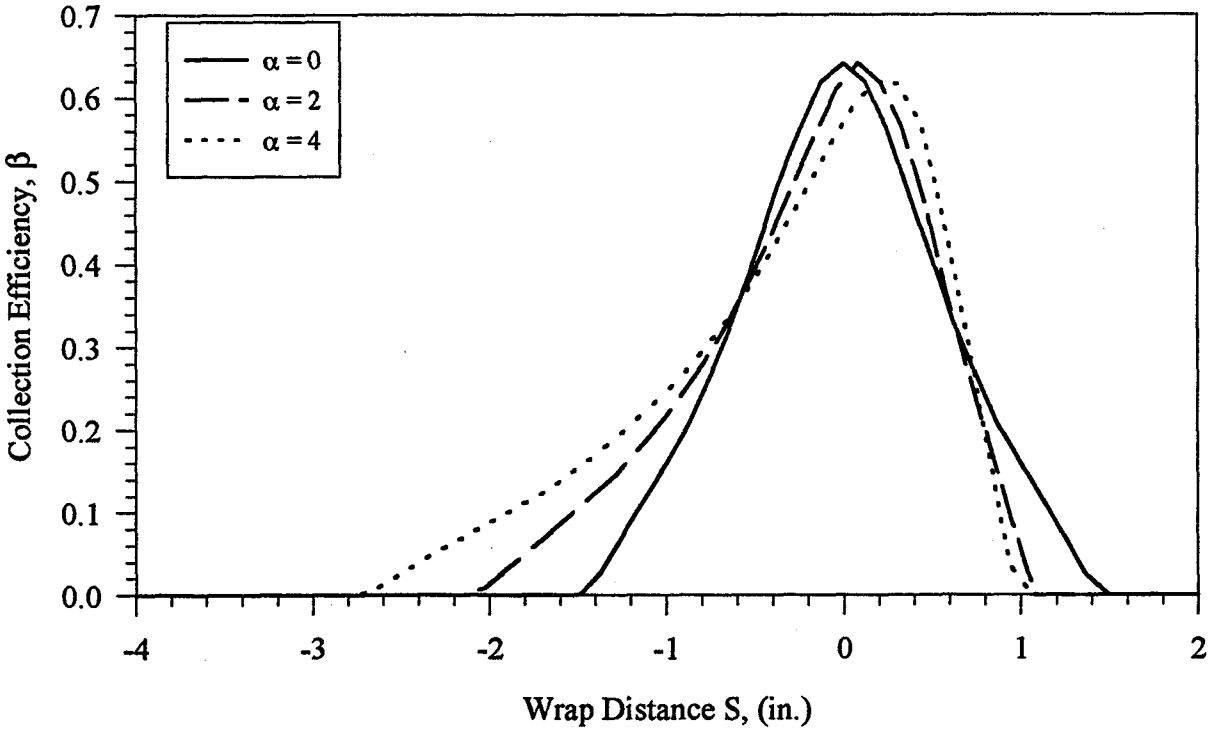

Figure 4a - Collection efficiency (β) for NACA-0012 airfoil.
(Droplet Diameter = 20μm, V = 100 mph)

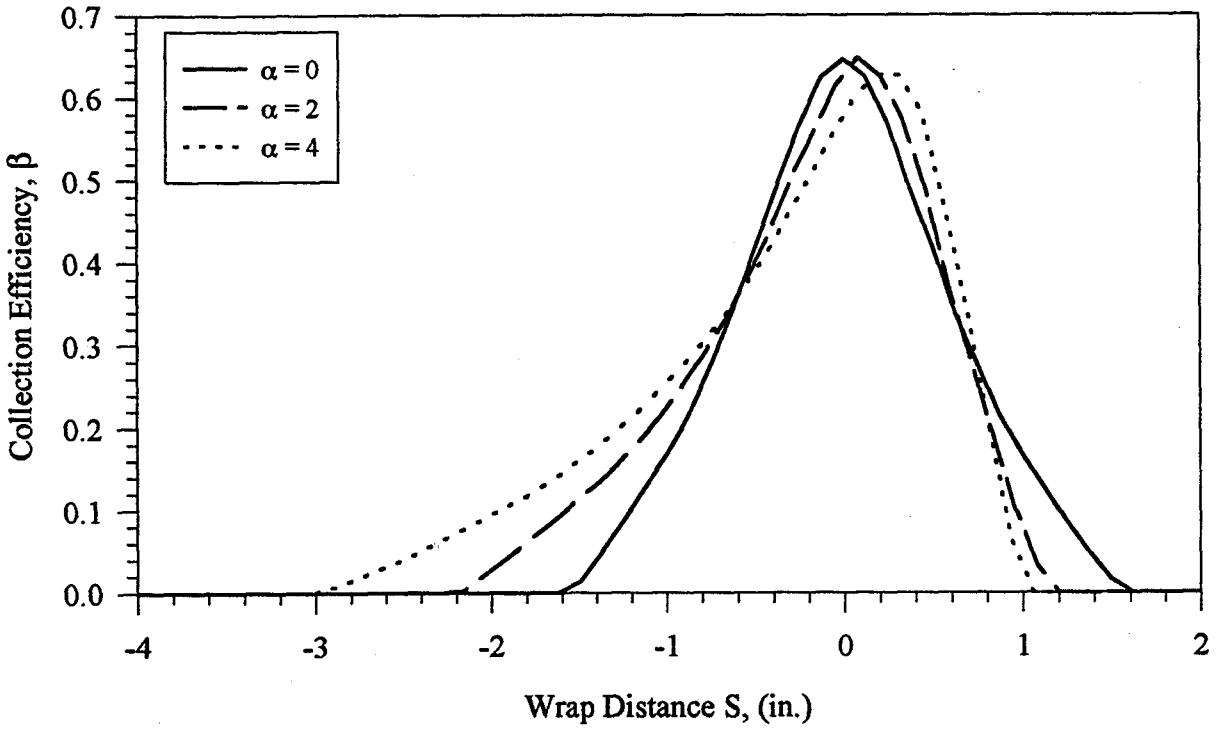

Figure 4b - Collection efficiency (β) for NACA-0012 airfoil. (Droplet Diameter = 20μm, V = 200 mph)

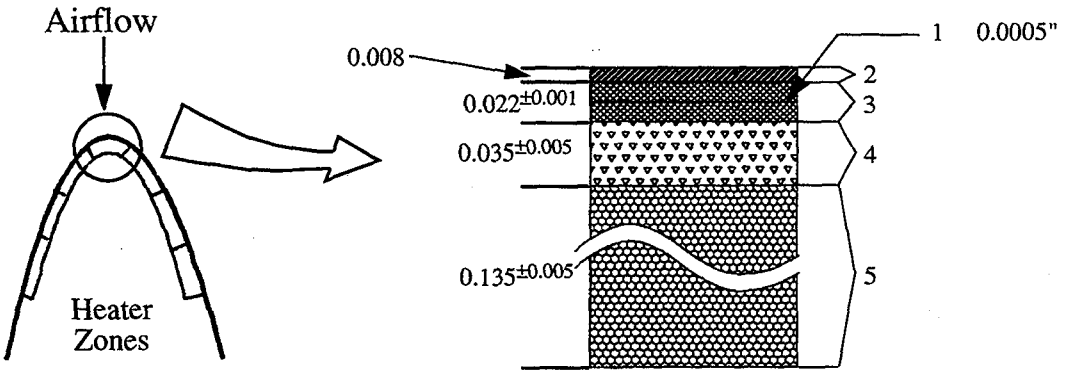

Item	Material	k (btu/hr.ft.F)	Density (lbm/ft^3)	Cp (Btu/lbm.F)
1	Heating Element (Alloy 90)	23.7	556	0.092
2	Erosion Shiled, SS 301 HH	9.4	501	0.12
3	Elastomer, COX 4300	0.148	86.4	0.30±0.03
4	Fiber Glass/Epoxy Composite	0.17	112	0.375
5	Silicone Foam Insulation	0.07	40.5	0.27±0.03

Figure 5 - Cross-sectional view of test article composite leading-edge.

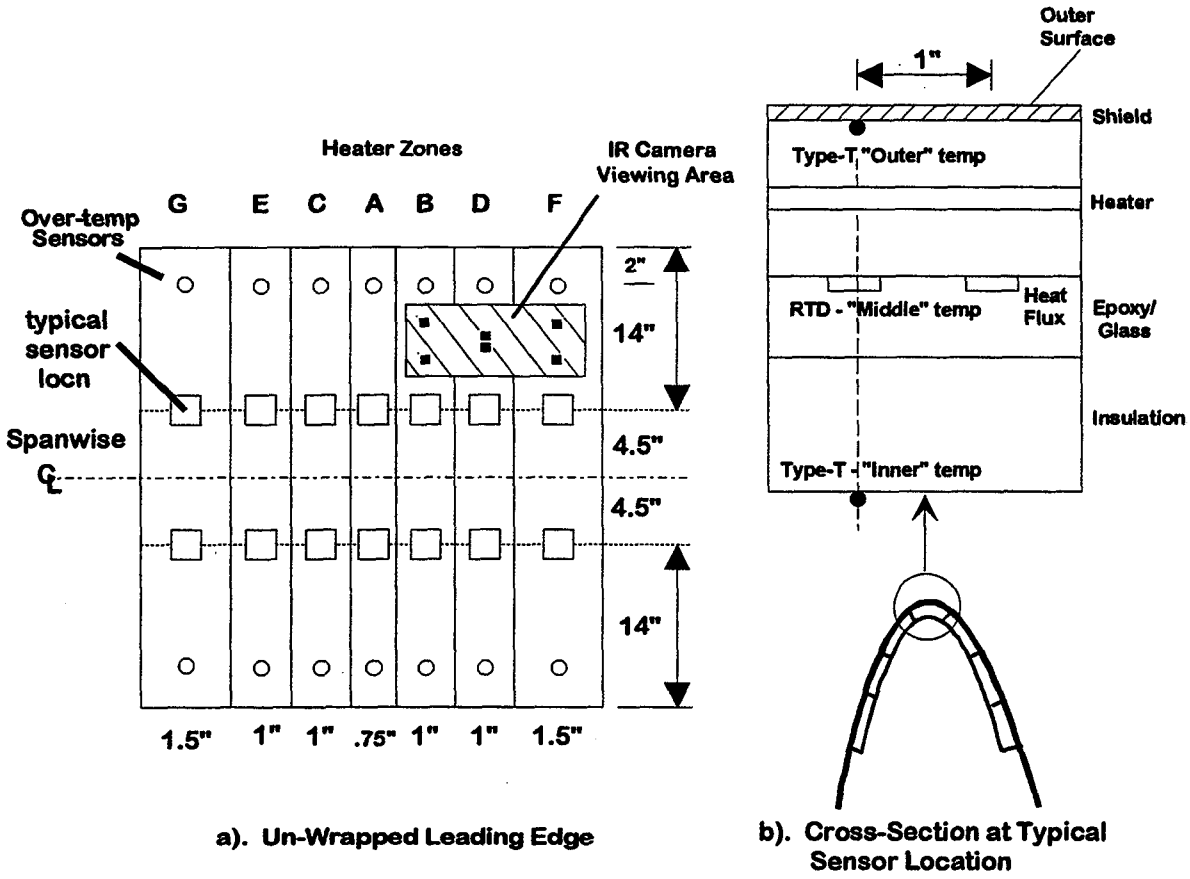

Figure 6 - Test article instrumentation layout.

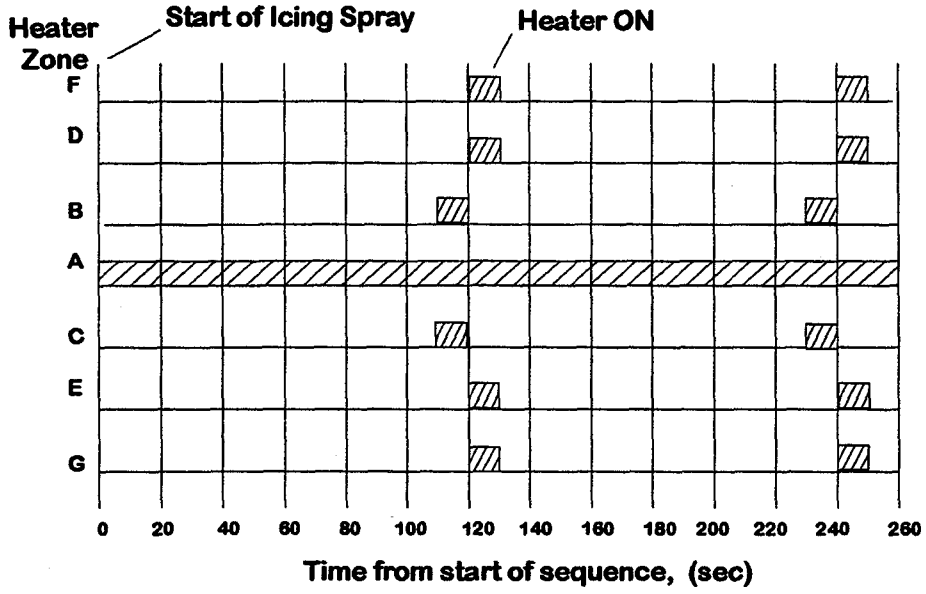

Figure 7 - Typical heater cycling sequence (10 sec heater ON/ 110 sec heater OFF)

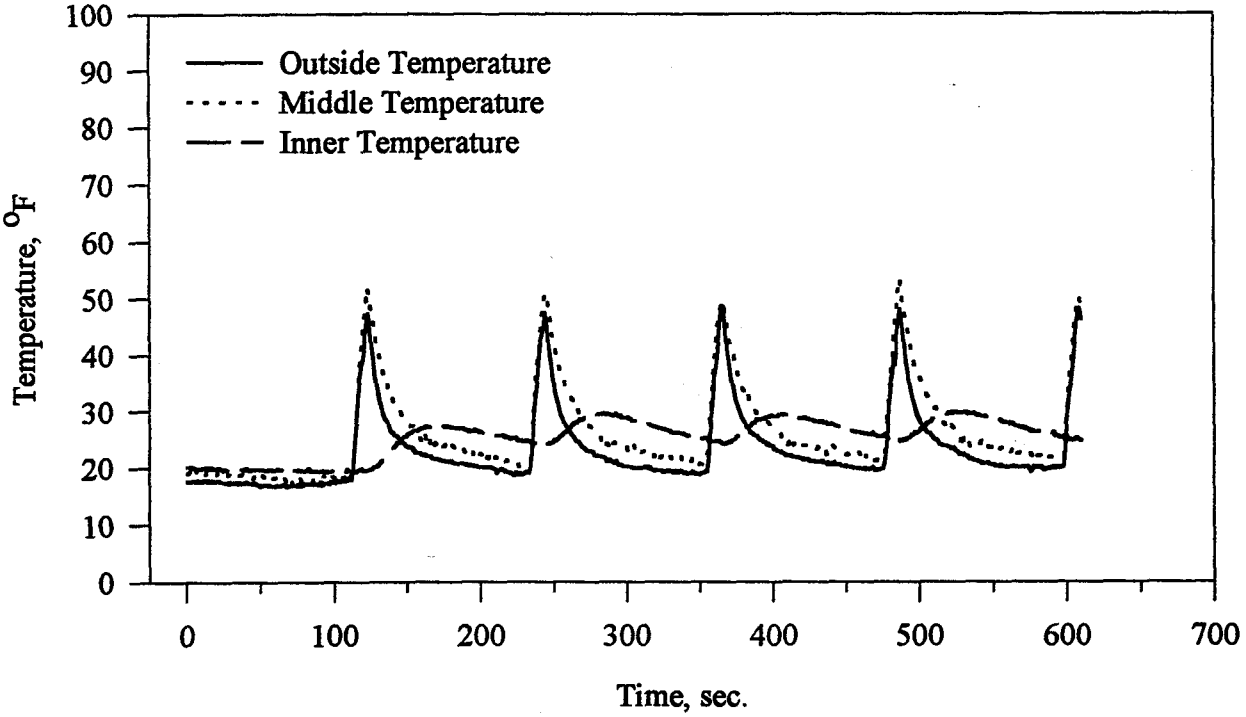

Figure 8 - Measured Temperature (De-Icing Run, Heater Zone F, NASA Run #28). Tt = 20°F, V = 100 mph, MVD = 20 um, LWC = 0.78 g/m^3, AOA = 0°

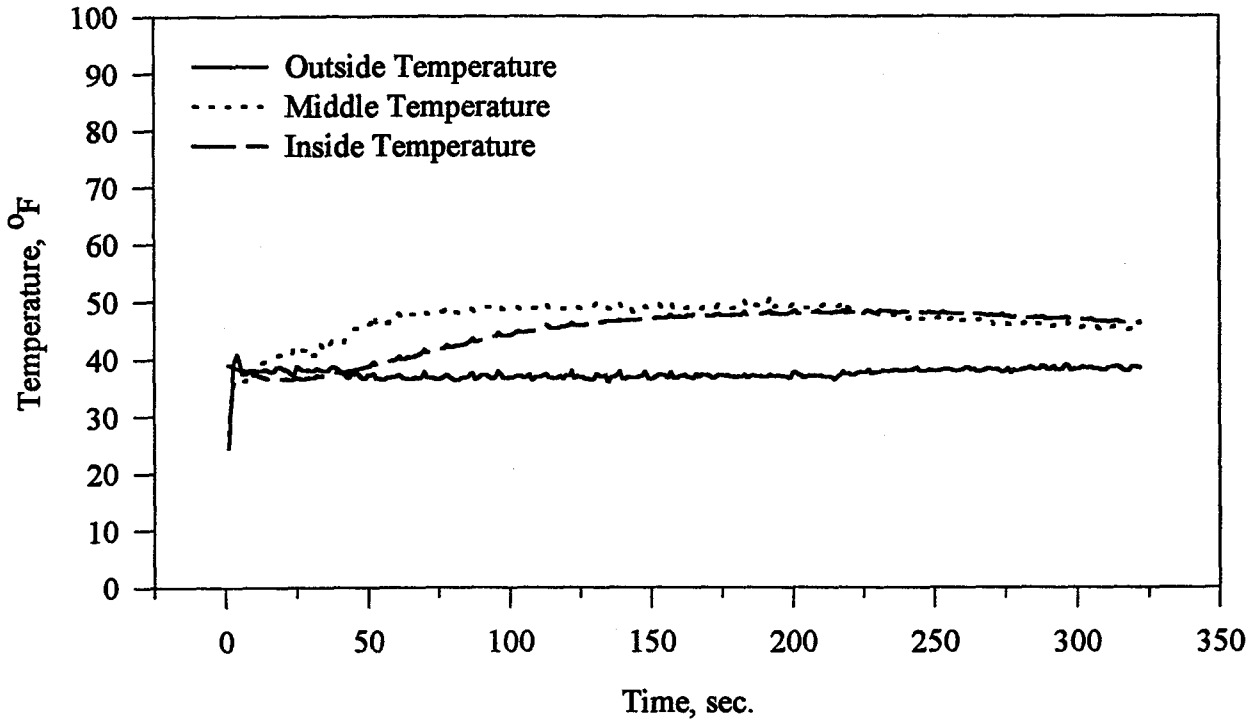

Figure 9 - Measured Temperature (Anti-Icing Run, Heater Zone A, NASA Run #22). Tt = 20°F, V = 100 mph, MVD = 20 um, LWC = 0.78 g/m^3, AOA = 0°

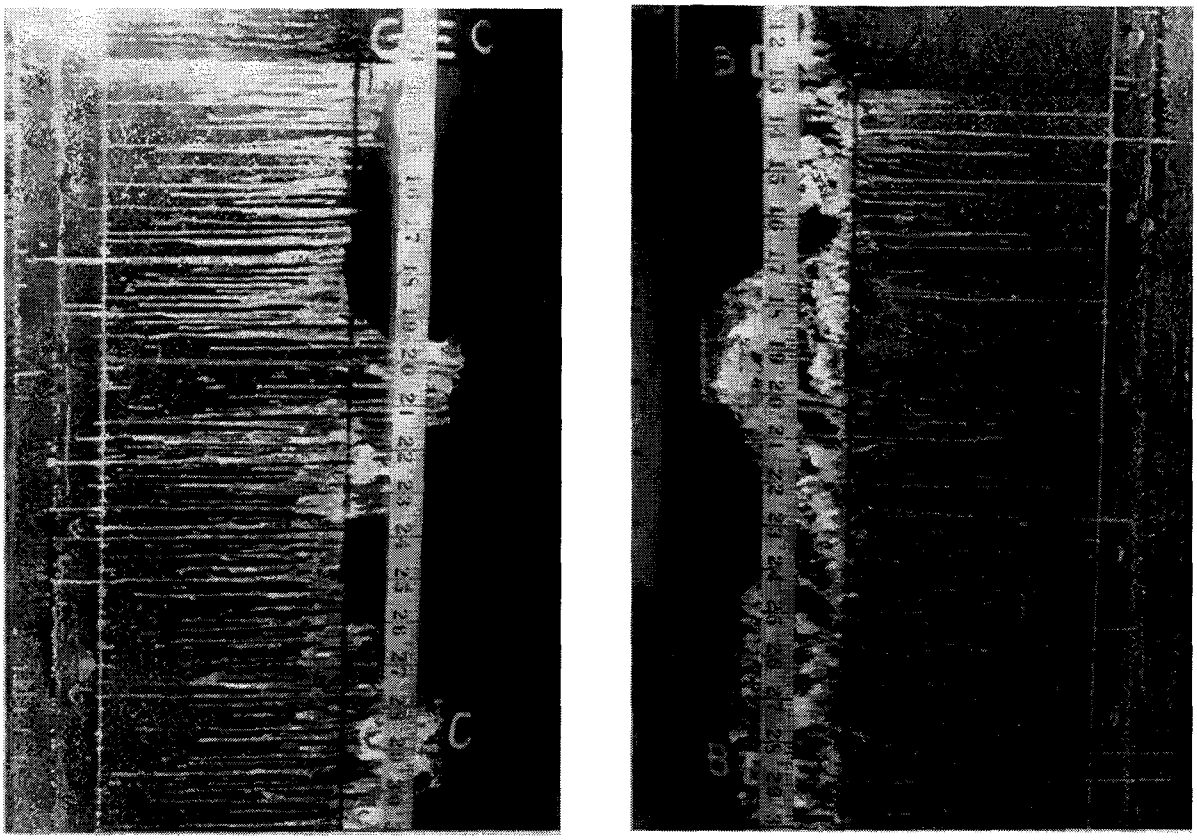

a). Run back aft of zones C, E and G.

b). Run back aft of zones B, D and F.

Figure 10 – Frozen runback on test article aft of heater zones.
(T_{tot} = 20°F, LWC = 1.1 g/m^3, MVD = 20 μm, V = 100 mph, AOA = 0°)

REPORT DOCUMENTATION PAGE

Form Approved
OMB No. 0704-0188

1. AGENCY USE ONLY (*Leave blank*)	2. REPORT DATE	3. REPORT TYPE AND DATES COVERED
	December 1996	Technical Memorandum

4. TITLE AND SUBTITLE

Validation of NASA Thermal Ice Protection Computer Codes
Part 1–Program Overview

5. FUNDING NUMBERS

WU–548–20–23

6. AUTHOR(S)

Dean Miller, Thomas Bond, David Sheldon, William Wright, Tammy Langhals, Kamel Al-Khalil, and Howard Broughton

7. PERFORMING ORGANIZATION NAME(S) AND ADDRESS(ES)

National Aeronautics and Space Administration
Lewis Research Center
Cleveland, Ohio 44135–3191

8. PERFORMING ORGANIZATION REPORT NUMBER

E–10602

9. SPONSORING/MONITORING AGENCY NAME(S) AND ADDRESS(ES)

National Aeronautics and Space Administration
Washington, DC 20546–0001

10. SPONSORING/MONITORING AGENCY REPORT NUMBER

NASA TM–107397
AIAA–97–0049

11. SUPPLEMENTARY NOTES

Prepared for the 35th Aerospace Sciences Meeting & Exhibit sponsored by the American Institute of Aeronautics and Astronautics, Reno, Nevada, January 6–10, 1997. Dean Miller, Thomas Bond, and David Sheldon, NASA Lewis Research Center; William Wright and Tammy Langhals, NYMA, Inc. 2001 Aerospace Parkway, Brook Park, Ohio 44142 (work funded by NASA Contract NAS3–17286); Kamel Al-Khalil, Cox & Company, Inc., New York, New York 10014; Howard Broughton, Cortez III Service Corporation, Cleveland, Ohio 44135. Responsible person, Dean Miller, organization code 5840, (216) 433–5349.

12a. DISTRIBUTION/AVAILABILITY STATEMENT

Unclassified - Unlimited
Subject Category 34

This publication is available from the NASA Center for AeroSpace Information, (301) 621–0390.

12b. DISTRIBUTION CODE

13. ABSTRACT ***(Maximum 200 words)***

The Icing Technology Branch at NASA Lewis has been involved in an effort to validate two thermal ice protection codes developed at the NASA Lewis Research Center. LEWICE/Thermal (electrothermal deicing & anti-icing), and ANTICE (hot-gas & electrothermal anti-icing). The Thermal Code Validation effort was designated as a priority during a 1994 "peer review" of the NASA Lewis Icing program, and was implemented as a cooperative effort with industry. During April 1996, the first of a series of experimental validation tests was conducted in the NASA Lewis Icing Research Tunnel (IRT). The purpose of the April 96 test was to validate the **electrothermal** predictive capabilities of both LEWICE/Thermal, and ANTICE. A heavily instrumented test article was designed and fabricated for this test, with the capability of simulating **electrothermal** de-icing and anti-icing modes of operation. Thermal measurements were then obtained over a range of test conditions, for comparison with analytical predictions. This paper will present an overview of the test, including a detailed description of (1) the validation process, (2) test article design, (3) test matrix development, and (4) test procedures. Selected experimental results will be presented for de-icing and anti-icing modes of operation. Finally, the status of the validation effort at this point will be summarized. Detailed comparisons between analytical predictions and experimental results are contained in the following two papers: "Validation of NASA Thermal Ice Protection Computer Codes: Part 2–The Validation of LEWICE/Thermal" and "Validation of NASA Thermal Ice Protection Computer Codes: Part 3–The Validation of ANTICE"

14. SUBJECT TERMS	15. NUMBER OF PAGES
Thermal; Ice protection; Anti-icing; De-icing	19
	16. PRICE CODE: A03

17. SECURITY CLASSIFICATION OF REPORT	18. SECURITY CLASSIFICATION OF THIS PAGE	19. SECURITY CLASSIFICATION OF ABSTRACT	20. LIMITATION OF ABSTRACT
Unclassified	Unclassified	Unclassified	